Self-affine crossover length in a layered silicate deposit

J. O. Fossum,* H. H. Bergene, Alex Hansen,† B. O'Rourke,‡ and G. Manificat
Department of Physics, The Norwegian University of Science and Technology, NTNU, N-7491 Trondheim, Norway
(Received 3 May 2002; revised manuscript received 15 August 2003; published 22 March 2004)

Self-affine dehydrated colloidal deposits on fresh mica surfaces of the synthetic layered silicate 2:1 smectite clay laponite have been studied by means of atomic force microscopy (AFM). AFM images of these prepared assemblies of sol and gel aggregates have been analyzed both by means of standard AFM Fourier software and a wavelet method. The deposited surfaces show a persistence to antipersistent crossover with a clay concentration dependent crossover length. It is concluded that the crossover length is associated with aggregate size, and further that the persistent roughness at small length scales signals near compact clusters of fractal dimension three, whereas the antipersistent roughness at large length scales signals a sedimentation process.

DOI: 10.1103/PhysRevE.69.036108 PACS number(s): 89.75.Fb, 68.35.Ct, 68.37.Ps, 91.60.−x

I. INTRODUCTION

Surfaces and profiles as characterized in terms of self-affinity are abundant in nature [1]. One class of natural surfaces, which has attracted considerable attention during a number of years, are those associated with surface growth [1,2], where several experimental and theoretical model systems have been studied [2].

Physical phenomena in clays represent a growing activity in the physics community [3,4]. All smectite 2:1 clays are polyelectrolytic inorganic colloids [5,6], whose primary particles are crystalline platelets with a thickness of about 1 nm. Most smectite clays have primary polydisperse platelet diameters in the micrometer range, whereas the most widely studied synthetic clay model system until now, laponite [7–9] is monodisperse with an aspect ratio of about 25 [7,8]. One has recently been able to establish the fundamental for a rich salt-clay concentration phase diagram of laponite, in which four dominant phases seem to govern the overall behavior at relatively low primary particle concentrations [8]: An isotropic liquid (IL) phase consisting of suspended aggregates of primary clay particles, an isotropic gel (IG) phase of percolating aggregation with fractal properties both dependant on salt-clay concentration and on time [8], a nematic gel (NG) phase for which excluded volume particle alignment has been proposed [10], and a flocculated (F) phase at high electrolyte concentrations.

The laponite arrives from the factory [7] in the form of a white powder, which is then mixed into salt water. Taking the added salt into account, dehydration from a given point in the phase diagram does not reverse the sample back into its initial powdery state. This is easily confirmed by macroscopic observations. atomic force microscopy (AFM) is a modern powerful imaging and analysis tool, which is generally utilized also in the characterization of clay minerals [11]. Surface topographies and roughness characteristics of natural cation-exchanged montmorillonite smectite clay films have already been studied by means of AFM (and optical microscopy) [12], and a direct correlation was found between the surface properties of the films, and those of the parent clay-electrolyte-water mix, and Hurst exponents ranging from 0.5 to 0.65 were reported, using standard image analyzing techniques.

Most AFM studies found in the literature have been performed by means of commercial ''off the shelf'' instruments, which arrive in the laboratory with the analyzing software included in the package. The digital instruments (DI) nanoscope AFM, which has been utilized during the present studies represents a good example of a very user friendly and excellent AFM imaging and analyzing tool. Power spectral density based methods are included in this commercial AFM software and may be utilized in order to study possible self-affine characteristics of imaged surfaces and profiles.

To our knowledge, no study has been done of a single system in which self-affine properties has been pretuned and designed by varying a controllable parameter. In the present case the actual phase diagram of laponite could possibly represent such a tunable parameter and we wanted to investigate these inherent possibilities.

The present paper is organized as follows: In Sec. II we describe sample preparation, and the AFM imaging. Section III deals with experimental results, and in Sec. IV the data are analyzed and discussed. Section V gives conclusions.

II. EXPERIMENTAL METHODS

With the ingredients summarized above in mind, we have deposited small samples originating from various parts of the laponite phase diagram onto cleanly cleaved mica surfaces. To prepare a sample, a freshly cleaved piece of mica was fastened on top of a 1-cm radius metal disk. Using a micropipette, a 10 μl drop of the sol or gel was placed on the mica surface. The drop was dispersed over the available area, and was then left to air dry for at least an hour, leaving dehydrated assembled rough films covering the mica surface. We imaged these surfaces using a DI AFM Multimode TM SPM with a nanoscope IIIa controller and a *J* scanner in tapping mode, which was chosen because contact mode proved to damage the clay films. Our AFM images are 10×10 or 2.5×2.5 μm^2 scans, and each image consists of the standard 512×512 pixels. The images were corrected for scanning curvature instrumental artifacts using the DI Nanoscope soft-

*Electronic address: jon.fossum@phys.ntnu.no
†Electronic address: Alex.Hansen@phys.ntnu.no
‡On exchange from Department of Pure and Applied Physics, Queens University Belfast, Belfast BT7 1NN, Northern Ireland.

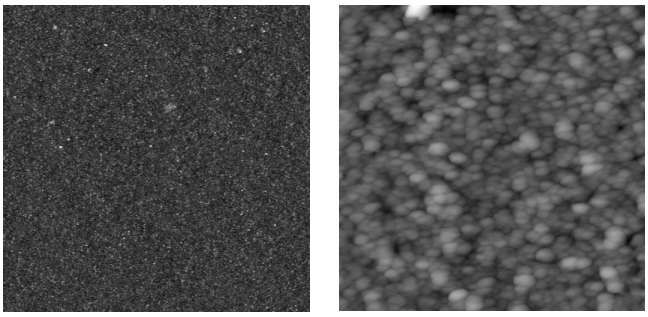

FIG. 1. Example AFM images (Sample 18). Scan sizes are 20 μm^2 (top) and 2 μm^2 (bottom). Figure 7 below shows typical cross sections of the present AFM images, i.e, the typical magnitude of the roughness, and thus illustrates the gray scale in these images.

ware flattening procedure. Finally the AFM images were analyzed by both using the standard DI AFM Fourier softwares and also by using the established wavelet methods [13,14].

Samples originating from different regions of the laponite phase diagram were deposited and imaged and results from two groups of samples studied are reported here: (1) 19 IL samples at clay concentrations ranging from 0.2 to 0.8 weight percent, and added NaCl salt concentrations at 0, 10^{-4}, and 10^{-3} mol/l. 2), four IG samples at 0.8 weight percent laponite, and NaCl concentrations ranging from 10^{-3} to 10^{-2} mol/l. The original samples belong to the same group of samples as reported earlier by Bakk *et al.* [18]. In the present paper we only include samples investigated by Bakk *et al* [18], since in these cases we have good estimates of aggregate sizes and resulting viscosities.

The present IL samples originate from a regime of linear viscosity (see Fig. 1 of Ref. [18]), whereas our IG samples originate from a regime of abrupt viscosity increase (at about 0.8 mol/l) [18]. The sol samples were Newtonian liquids and the gel samples had finite Bingham thresholds [18] at the time of deposition.

In preparing the present samples as desrcribed by Bakk *et al.* [18], the pH of all solutions was adjusted to about 10 prior to laponite hydration in order to prevent initial primary particle dissolution [8], and the samples were then left for several months before viscosity measurements and the final dispersion on top of the fresh mica surfaces was performed as described above. It is important to note that the samples were not completely sealed from exposure to air during this time of storage, thus no attempt was made to prevent pH driven particle dissolution, and subsequent Mg^{2+} contamination [15]. This is an important point since our gel samples ''should not have been gels'' according to the laponite phase diagram without this contamination [8,15]. It is also reasonable to assume that our sol samples contained dissolved Mg^{2+} ions for the same reason. Only two of the gel samples were analyzed by means of Hurst exponents and crossover lengths [16].

III. EXPERIMENTAL RESULTS

Figure 1 shows typical AFM images for one of our rough surfaces originating from deposition of one of our IL samples (sample 18).

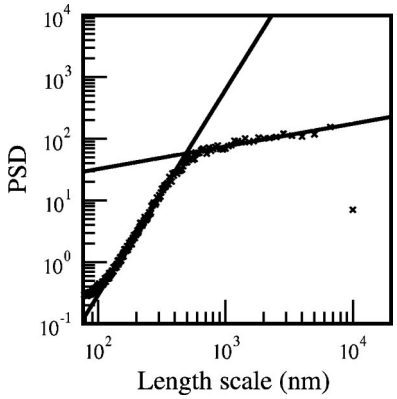

FIG. 2. Power spectrum of sample 2D showing Hurst exponents $H=1.16$ and $H=-0.32$.

One representative example of a DI software based two-dimensional power spectrum from one of the present AFM images is shown in Fig. 2. The spectrum consists of two power laws. The exponents of the power laws b are related to the Hurst exponents of the surfaces, H, as $b=2H+1$ [17]. A crossover length L_c is easily defined through the scale at which one power law changes into another one. Actually all our imaged samples indicate such a crossover from a large Hurst exponent at small length scales to a small Hurst exponent at larger scales. But in order to investigate the crossover, the samples have to be imaged at scan sizes larger than the crossover length. Unfortunately only two of the gel images are good enough for analyzing. Therefore gels may be worth closer investigation with respect to crossover length and Hurst exponents. This will be a topic for further studies.

In fact, a close examination of Fig. 2 indicates a second crossover at the smallest length scale, where the power spectrum becomes flat. We believe that this second crossover is due to the onset of finite tip size effects. Thus, the flat region of the power spectrum at length scales below 12 nm results from a convolution of the actual physical surface and our AFM tip, which in this case would have a radius of about 12 nm, a normal curvature for such commercial tips. Furthermore, we observe in Fig. 6 that the amplitude of the observed surface roughness is about the same as the observed tip radius. Thus, we believe that our tip is well suited for mapping

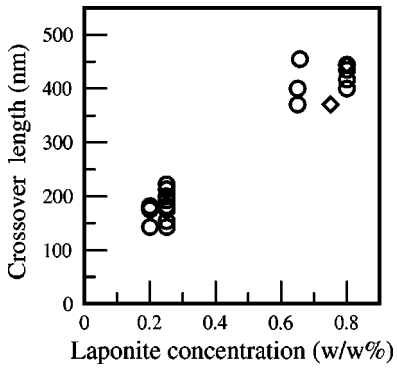

FIG. 3. Crossover length based on power spectra such as the one in Fig. 2 vs laponite concentration. (o) are solutions and ($\diamond$) are gels.

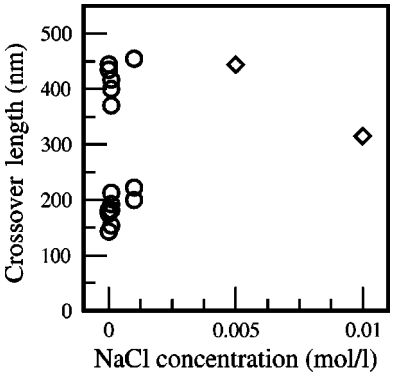

FIG. 4. Crossover length based on power spectra such as the one in Fig. 2 vs NaCl concentration. (o) are solutions and ($\diamond$) are gels.

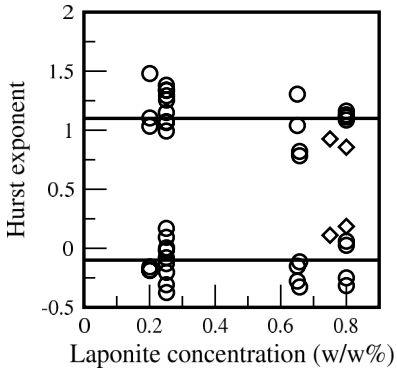

FIG. 5. Hurst exponents based on power spectra vs laponite concentration. Solid lines denote the average of Hurst exponents at small and large length scales at respectively $H=1.1$ and $H=-0.1$. (o) are solutions and ($\diamond$) are gels.

out such surfaces at length scales above 12 nm.

Figures 3–5 summarize results of our present AFM imaging: Fig. 3 shows evidence of a correlation of the crossover length versus the laponite concentration, Fig. 4 indicates that there is no correlation between the crossover length and NaCl concentration, and Fig. 5 shows the two observed Hurst exponent regimes versus laponite concentration, giving an average value of $H\sim 1.1$ for small length scales, and $H\sim -0.1$ for large length scales. The qualitative difference between the two regimes is shown in Fig. 6, where a 512 pixel trace across one of our imaged surfaces is shown. Simultaneous antipersistent behavior at short length scales and persistent behavior at large length scales are evident.

A comment is appropriate here. Figure 7 shows data for one of the given samples, using wavelet analysis. The same goes for Fig. 2, but here power spectrum analysis is used. Figure 5, on the other hand, collects the power spectrum data from all samples. The data of Fig. 2 are embedded in this figure. There are large sample to sample variations, which is reflected in the value $H=0.3$ for the samples in Figs. 2 and 7 being so different from the average value $H=-0.1$.

Hurst exponents are also found using the method of averaged wavelet coefficients (AWC) [14]. This method confirms the results of the power spectrum method, giving $H\sim 1$ and $H\sim 0$. Figure 7 shows an AWC equivalent of a power spectrum like the one shown in Fig. 2 for three different wavelet filter coefficients.

IV. ANALYSIS AND DISCUSSION

The appearance of two different scaling regimes signals that two physical processes have been involved. The surfaces have been produced by a sedimentation process of clay platelet clusters, which has been followed by the passage of the water meniscus through the surface.

At large length scales, we essentially see the results of the sedimentation process, and a Hurst exponent of essentially zero signals a logarithmically rough surface. This is consistent with the annealed-disorder Edwards-Wilkinson (EW) growth equation in $(2+1)$ dimensions [2]. We would expect this growth equation rather than the Kardar-Parisi-Zhang (KPZ) equation [2] to be the relevant one here as the nonlinear term that separates the KPZ equation from the EW equation, which is due to the change in flux normal to the local surface of the deposit as a result of its orientation with respect to the vertical direction, is washed out due to Brownian movement of the depositing clusters. It is thus worth commenting that a Hurst exponent of zero does not signal random noise, but logarithmic roughness. Random noise would give a Hurst exponent of -0.5 as discussed by Hansen *et al.* [19]

At smaller length scales, the observed roughness presumably is a result of the collapsing of the clay clusters due to the passing of the water meniscus. This is supported by the fact that our own AFM images of very dilute sol samples, for which isolated aggregates can be seen, suggest considerable vertical collapse as water is removed. The observed Hurst exponent of the surface reflects the structure of the clusters before they collapse. This may be understood as follows: A fractal structure in three-dimensions is projected onto a two-dimensional plane. The height of the projected structure at a

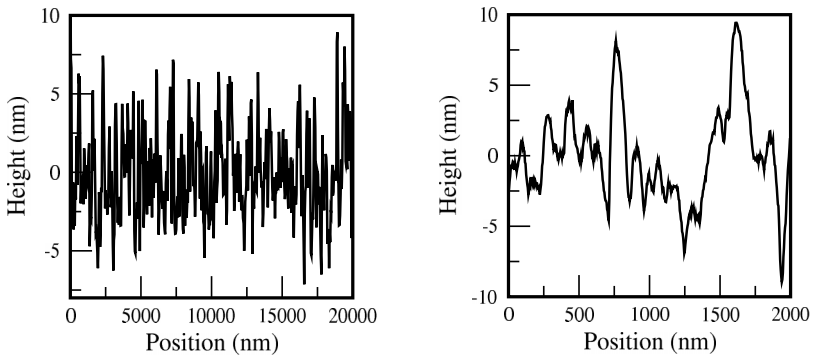

FIG. 6. Cross sections of images shown in Fig. 1. Note, the antipersistent behavior at large length scale (left) and the persistent behavior at small length scale (right).

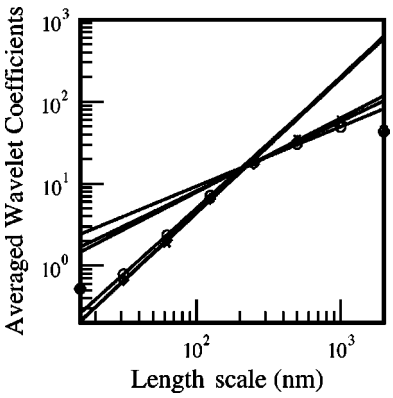

FIG. 7. Averaged Wavelet Coefficients vs length scale. Wavelet coefficients used are Daubechies 4(o), 12($\diamond$), and 20(x), giving $H=1.11\pm0.03$ and $H=0.3\pm0.1$ (Sample 28).

given point is proportional to the fractal sitting above this point. All our AFM images are taken with a pixel size well above the individual laponite particle size, which is about 1×25 nm. Thus, at our smallest length scales we always measure collapsed clusters of such individual particles, and the measured Hurst exponent H at small length scales, thus, tells us something about the structure of clusters before collapse. It can be shown that the Hurst exponent of a collapsed structure H is related to the fractal dimension of an uncollapsed structure D by the equation $D=2+H$. Hence, when we find a Hurst exponent of one this tells us that the fractal dimension of the suspended and uncollapsed clusters is three.

We note that another system showing a crossover between two scaling regimes is recently reported in stylolites (irregular rock-rock interface zones) [20].

We note that neither the clay particle concentration nor the electrolyte concentration seem to play a significant role as far as Hurst exponents for the samples investigated in this study are concerned and that apparently only the clay concentration increase seems to influence the crossover lengths. This latter observation is in good agreement with the parent phase diagram [8] in which the IL-IG transition line is nearly salt independent below 10^{-3} mol/l NaCl concentrations, and it is also in agreement with our own relative viscosity data from the same original samples [18].

The transient birefringence data of Ref. [18] do suggest electrolyte dependent aggregate structures/sizes in aqueous solutions. This is not in contradiction to the present observations since salt should play an important role only in the presence of water, and our observed crossover lengths thus reflect the number of clay particles in a given collapsed (projected) aggregate and their shape.

V. CONCLUSIONS

From above we are led to the following conclusions: (1) crossover length is associated with aggregate size in agreement with Ref. [18]; (2) at small length scales $H\sim1$, signaling that the clusters have fractal dimension three; (3) $H\sim0$ at large length scales may signal a sedimentation process that follows the Edwards-Wilkinson equation, and hence the roughness is logarithmic.

ACKNOWLEDGMENTS

This research was supported by NTNU/NFR SUP Grant No. 115185/420 during the early stages. B. O'Rourke and J. O. Fossum wish to acknowledge Sintef Petroleum Technology for partial support.

[1] J-F. Gouyet, *Physics and Fractal Structures* (Masson, Paris, 1996).
[2] A.-L. Barabasi and H.E. Stanley, *Fractal Concepts in Surface Growth* (Cambridge University Press, Cambridge, UK, 1995).
[3] H. van Damme, C. R. Acad. Sci. Paris t. 320 serie IIa, 665 (1995).
[4] J.O. Fossum, *Complex Physical Phenomena in Clays*, edited by A.T. Skjeltorp and D. Sherrington, Soft Condensed Matter: Configurations, Dynamics, and Functionality (Kluwer Academic, Amsterdam, 2000).
[5] B. Velde, *Introduction to Clay Minerals* (Chapman and Hall, London, 1992).
[6] H. van Olphen, *Clay Colloid Chemistry*, 2nd ed. (Krieger Puplishing Company, Florida, 1991).
[7] P.K. Jennes, Laporte Absorbents, U.K. technical reports (unpublished).
[8] A. Mourchid, E. Lecolier, H. van Damme, P. Levitz, Langmuir **14**, 4718 (1998).
[9] R.J.F. Leote de Carvalho, E. Trizac, and J-P. Hansen, Europhys. Lett. **43**, 369 (1998).
[10] J.P. Gabriel, C. Sanchez, and P. Davidson, J. Phys. Chem. **100**, 11139 (1996).
[11] *Scanning Probe Microscopy of Clay Minerals*, edited by K.L. Nagy and A.E. Blum, CMS Workshop Lectures Vol. 7 (The Clay Minerals Society, Boulder, 1994).
[12] M. Zabat, M. Vayer-Besancon, R. Harba, S. Bonnamy, and H. van Damme, Prog. Colloid Polym. Sci. **105**, 96 (1997).
[13] A.R. Mehrabi, H. Rassamdana, and M. Sahimi, Phys. Rev. E **56**, 712 (1997).
[14] I. Simonsen, A. Hansen, and O.M. Nes, Phys. Rev. E **58**, 2779 (1998).
[15] A. Mourchid and P. Levitz, Phys. Rev. E **57**, R4887 (1998).
[16] M. Reiner, *Deformation, Strain and Flow*, H.K. Lewis CO. LTD. London (1969).
[17] A. Hansen, K.J. Måløy, and T. Engøy, Fractals **2**, 527 (1994).
[18] A. Bakk, J.O. Fossum, G.J. da Silva, H.M. Adland, A. Mikkelsen, and A. Elgsater, Phys. Rev. E **65**, 021407 (2002).
[19] A. Hansen, J. Schmittbuhl, and G.G. Batrouni, Phys. Rev. E **63**, 062102 (2001).
[20] J. Schmittbuhl, F. Renard, and J.P. Gratier, presented at 27th General Assembly of the European Geophysical Society, Nice, France 21-26 April 2002, Geophysical Research Abstracts, Volume 4, NP9. 01, NP006; EGS02-05508; NP9.01-1MO5P-006 (2002).